Proton Radiation Effects on Hamamatsu InGaAs PIN Photodiodes

Raichelle Aniceto, Randall Milanowski, Slaven Moro, Kerri Cahoy, and Garrett Schlenvogt

***Abstract*—Hamamatsu InGaAs PIN photodiodes were exposed to 105 MeV protons to a fluence of 2.55×10^{11} p/cm^2. Radiation induced increase in dark current was observed that appeared stable following room temperature annealing. A preliminary TCAD model was developed for use in mixed-mode simulation analyses**

I. INTRODUCTION

PROTON radiation effects in Hamamatsu InGaAs PIN photodiodes are examined along with simulated radiation response of the photodiodes using defect-based TCAD modeling. The devices under test (DUTs) were low noise, high reliability quadrant-type InGaAs PIN photodiodes manufactured by Hamamatsu (G6849-01). The photodiodes have 1 mm diameter active areas and are suited for 1550 nm applications. Each quadrant-type photodiode has 4 PIN diodes. Typical reverse bias voltage for the photodiodes is 1V. Dark current values can reach up to 1.5 nA, but the typical dark current value is 0.15 nA [1].

One radiation test campaign was conducted at TRIUMF National Laboratory with proton energy level of 105 MeV and fluence levels between 5.0×10^9 and 2.55×10^{11} p/cm^2. The dark current and responsivity of the photodiodes were measured prior to and after proton irradiation. The experimental results were compared to TCAD simulations of the PDs to determine the amount of majority and minority trap densities that could be correlated to the observed radiation effects.

Displacement damage from proton irradiation leads to increased dark current and degraded responsivity in InGaAs photodiodes due to the generation of defect traps and recombination centers in the active region. A study on proton irradiation of InGaAs PIN photodiodes by Barde et al. (2000) observed an overall 10 to 1000-fold increase in dark current values from proton irradiation with energy levels between 9 and 300 MeV and fluences between 2×10^9 and 10^{10} p/cm^2. This study found a linear relationship between dark current and proton fluence [2]. Another study by Troska et al. (1997) observed a non-linear increase of 6 to 7 orders of magnitude in dark current of InGaAs PIN PDs from 24 GeV proton irradiation with fluence levels of 4×10^{14} and 10^{15} p/cm^2. This study also found a 10% decrease in photocurrent for fluences up to 10^{13} p/cm^2, but responsivity rapidly approached zero for higher fluences [3]. We will evaluate if our experimental results show similar behavior with these previous studies, and our experimental findings will also be used to estimate the amount of trap densities in the photodiode active regions that could yield similar displacement damage effects to the experimental results.

We expect that these results will be of use to the satellite and aerospace industries and will move forward Facebook's mission of connectivity.

II. EXPERIMENTAL

The proton test campaign was conducted on a group of four DUTs irradiated with 105 MeV proton energy level. One of the DUTs (DUT#4) was irradiated to a total of six proton fluence levels of 5.0×10^9 p/cm^2, 1.5×10^{10} p/cm^2, 3.3×10^{10} p/cm^2, 8.0×10^{10} p/cm^2, 1.67×10^{11} p/cm^2, and 2.55×10^{11} p/cm^2. The remaining three DUTs were irradiated to only the three highest proton fluence levels of 8.0×10^{10} p/cm^2, 1.67×10^{11} p/cm^2, and 2.55×10^{11} p/cm^2. The dark current values were measured prior to proton irradiation and after each round proton irradiation to the specified fluence levels. Two sets of post proton irradiation anneal data were collected: Anneal 1 data was collected after a 24-hour time period at TRIUMF and Anneal 2 data was collected after a time period of 56 days. The DUTs were unbiased and stored in room temperature during the anneal period.

An Agilent B1505A semiconductor parameter analyzer was used to conduct the measurements of the photodiodes. The DUT was placed inside the slit of a dark block of foam during dark current measurements to shield ambient light. Figure 1 shows the measurement setup with the parameter analyzer and DUT placed inside slit of dark block of foam.

Manuscript received September 29th, 2017. This work was supported by the Facebook Connectivity Lab.

Raichelle Aniceto is with Facebook. 1 Hacker Way, Menlo Park, CA 94025 USA (telephone: +1-801-859-719, e-mail: raniceto@fb.com).

Randall Milanowski is with M&A, Inc., 2726 Shelter Island Drive #268, San Diego, CA, 92106 USA (telephone: +1-619-865-2174, email: rmilanowski@radhard.com).

Slaven Moro is with Facebook. 1 Hacker Way, Menlo Park, CA, 94025 USA (telephone: +1-619-300-9204, e-mail: smoro@fb.com).

Kerri Cahoy is with MIT, 77 Massachusetts Ave. Cambridge, MA 02139 USA (telephone: +1-650-814-8148, email: kcahoy@mit.edu).

Garret Schlenvogt is with Silvaco, 7 Technology Dr. North Chelmsford, MA, 01863 USA (telephone: +1-978-322-9930, email: garrett.schlenvogt@silvaco.com).

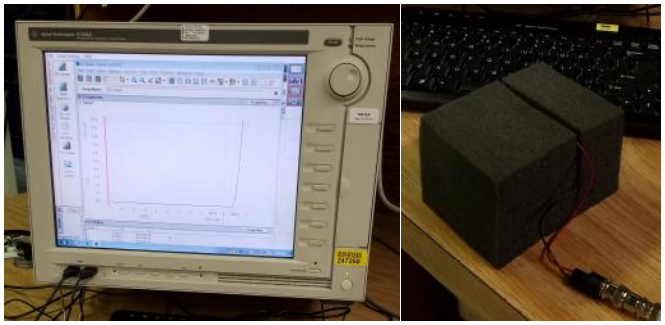

Fig. 1. Photodiode measurement setup showing the Agilent B1505A semiconductor parameter analyzer (left) used to conduct pre and post radiation photodiode measurements and the block of foam (right) used to shield DUT from ambient light during measurements.

Dark current measurements were collected for each of the 4 pin diodes within a photodiode, and the average dark current value of the photodiode was calculated as the average dark current of the 4 pin diodes. For proton irradiation, the group of photodiodes were mounted to a test board (Figure 2 (Top)). A laser was used to align the proton beam with the DUTs. Figure 2 (Bottom) shows the proton irradiation test setup with the proton beam port and mounted photodiodes.

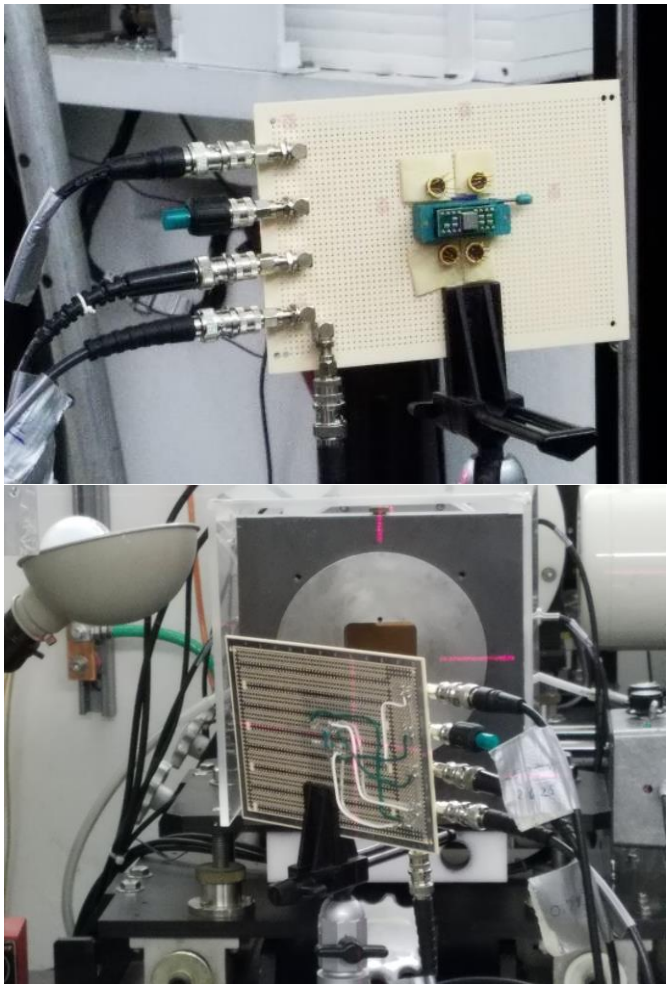

Fig. 2. Proton radiation test setup; (Top) 4 DUTs mounted onto test board during proton irradiation; (Bottom) Photodiode test board aligned to proton beam

III. Results

DUT #4 I-V curves were generated from the average pre and post proton irradiation dark current measurements of the 4 pin diodes within the DUT (Figure 3). Due to noise in our parametric measurement setup at the proton test facility, our pre-rad measurements show unrealistically large reverse leakage values, e.g., several nanoamps (considerably higher than the nominal 0.15 nA reverse leakage in the product datasheet). The reverse dark currents increased rapidly with proton fluence and so noise was not a factor in the post-exposure data.

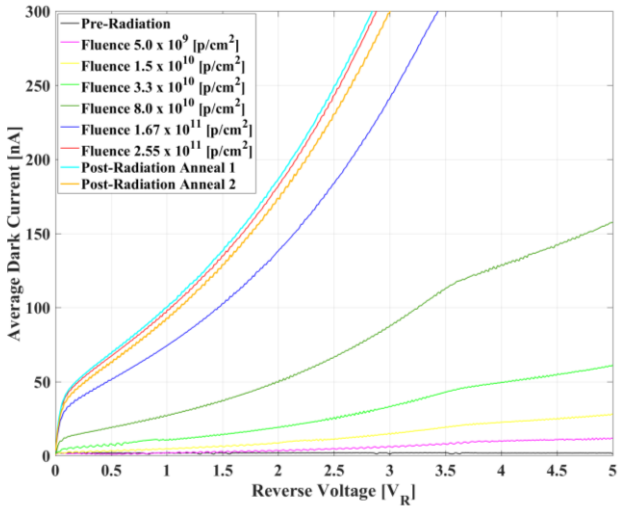

Fig. 3. DUT #4 I-V curves from average pre and post proton irradiation dark current measurements

The average dark current values for 1V reverse voltage level were analyzed for the pre and post irradiation measurements (Figure 4). The calculated dark current average standard deviation values at 1V reverse voltage level for the pre and post irradiation fluence levels are shown in Table I.

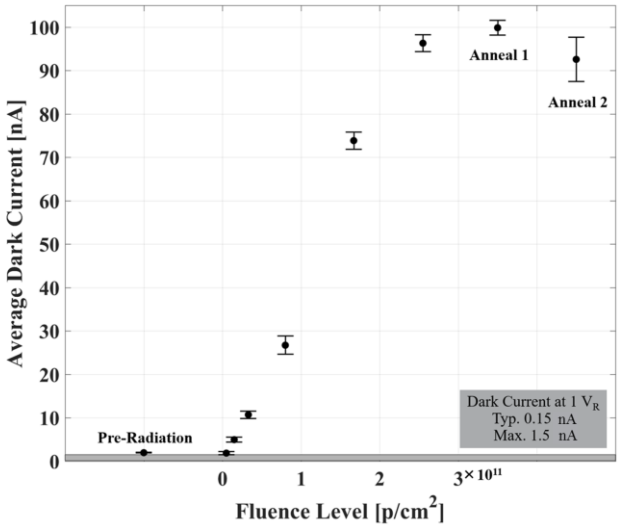

Fig. 4. DUT #4 average dark current values at 1 V_R from pre and post irradiation measurements. The typical and maximum dark current values at 1V reverse voltage from part specification indicated.

TABLE I. DUT #4 Dark Current Measurements at 1V Reverse Voltage

Fluence Level [p/cm^2]	μ Dark Current [nA]	σ Dark Current [nA]
Pre-Radiation	1.97	0.07
5.0×10^{9}	1.87	0.37
1.5×10^{10}	4.97	0.57
3.3×10^{10}	10.71	0.87
8.0×10^{10}	26.73	2.11
1.7×10^{11}	73.85	2.00
2.6×10^{11}	96.30	1.95
Anneal 1	99.85	1.70
Anneal 2	92.58	5.09

The dark current measurements among all four DUTs were averaged to generate summary pre and post proton irradiation I-V curves for the 3 common fluence levels (Figure 5). Similar to the observations for DUT #4, as proton fluence levels increased within each test campaign, the current values increased for a given reverse voltage. Thus an increasing trend in the I-V curves was seen in the experimental results of a given test campaign. As proton fluence level increased, the photodiode dark current at 1V reverse voltage linearly increased for a given test campaign. Figure 6 displays the relationship between proton fluence and photodiode dark current at 1V reverse voltage from the experimental results. Table II summarizes lists experimental results for the pre and post proton irradiation average photodiode dark current values at 1V reverse voltage for each group of photodiodes.

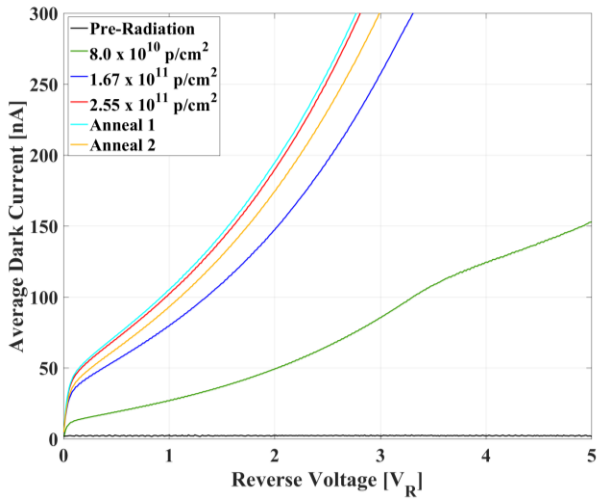

Fig. 5. I-V curves from pre and post proton irradiation dark current measurements averaged among all 4 DUTs.

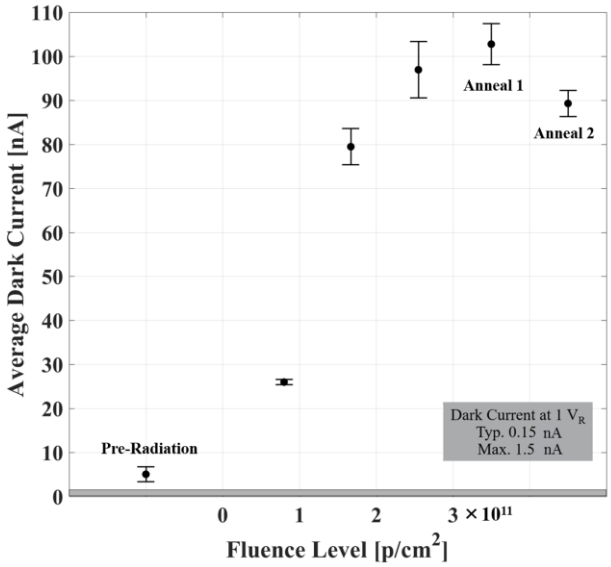

Fig. 6. Average dark current values at 1V reverse voltage from pre and post irradiation measurements among all 4 DUTs. The typical and maximum dark current values at 1V reverse voltage from part specification indicated.

TABLE II. Average Dark Current Measurements at 1V Reverse Voltage for all DUTs

Fluence Level [p/cm^2]	μ Dark Current [nA]	σ Dark Current [nA]
Pre-Radiation	5.05	1.66
8.0×10^{10}	25.98	0.60
1.7×10^{11}	79.45	4.11
2.6×10^{11}	96.93	6.41
Anneal 1	102.75	4.70
Anneal 2	89.28	2.98

IV. DISCUSSION

The results were evaluated for potential space mission applications. The OMERE radiation environment modeling program was used to simulate the expected trapped proton integral flux for 105 MeV protons with trapped proton model AP8-MIN and IGRF magnetic field model. Based on OMERE simulations for a 1-year mission duration, the maximum proton fluence level for 105 MeV protons is ~5.5×10^{10} p/cm^2 for a 500 km orbit altitude and ~1.5×10^{11} p/cm^2 for a 1000 km orbit altitude. Correlated with DUT #4 dark current results, we would expect to see an average dark current value between 10.71 nA and 26.73 nA at $1V_R$ for the 500 km orbit altitude and an average dark current value between 26.73 nA and 73.85 nA at $1V_R$ for the 1000 km orbit altitude after 1-year mission durations. Based on the results of increased dark current with proton fluence, InGaAs PIN photodiode degradation due to proton radiation could be significant for 1 year missions.

Shielding could be used to mitigate proton radiation effects, but effective shielding material and thickness will be based on the environment, i.e. proton energy spectrum. Circuit level processing could potentially be configured to be tolerant of gradual dark current and responsivity degradation.

V. Device Simulations

A preliminary device simulation analysis was initiated to examine how radiation induced defect properties and device structural details influence InGaAs PIN diode parametric degradation. The model structure we are using is based on the discussion in [4] and is shown schematically in Figure 7(a). Figure 7(b) shows the corresponding structure created using the ATLAS device simulator. Note that we do not have detailed structural information on the devices we radiation tested, so our simulation results are qualitative. We did however scale the x and effective z dimensions of the model structure to match the active area of the experimental devices.

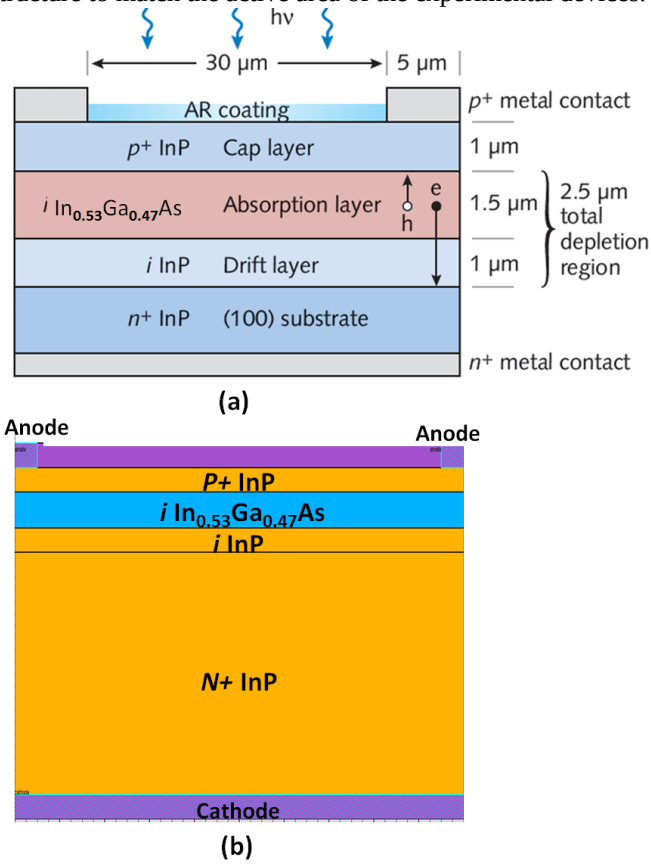

Fig. 7. (a) A cross-section shows the top-illuminated indium gallium arsenide (InGaAs) dual-depletion region (DDR) epitaxial structure of the highly linear photodiode (HLPD) device. (b) Cross section view of the device simulation structure.

Simulated IV curves for dark and illuminated (1.55 μm wavelength) conditions are shown for a pre-radiation structure in Fig. 8 and a post-radiation structure in Fig. 9. The proton-induced displacement damage is represented with a spatially uniform distribution of trap levels with a density of 1×10^{11} traps/cm^3 for the InP and InGaAs regions. The energy level of the traps are chosen to be at midgap, which maximizes their effect on recombination rate. Figure 9 shows the expected increase in dark current and decrease in photogenerated currents under reverse bias. The simulated increase in dark current roughly corresponds to the 100nA value observed for experimentally for the 2.55×10^{11} proton/cm^2 fluence. The simulation also predicts a radiation-induced decrease in the photovoltage of the illuminated diode characteristic. Figures 10 and 11 show the same data as Figures 8 and 9 with the anode currents displayed on a linear scale.

The decrease in responsivity is also shown in the pre-radiation and post-radiation plots of cathode current vs. optical wavelength in Figure 12.

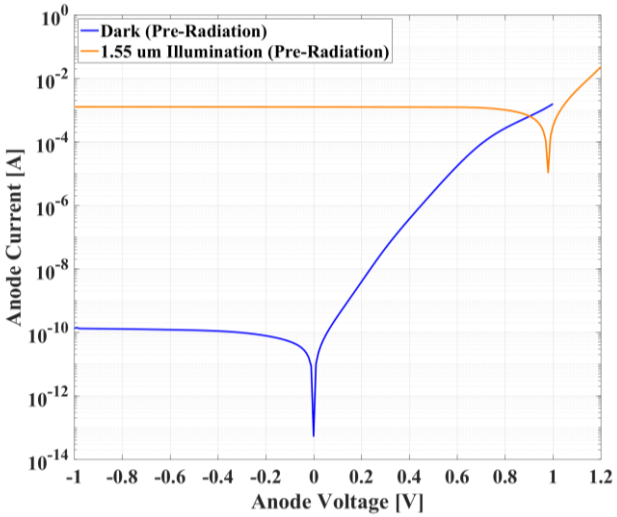

Fig. 8. Simulated dark and illuminated IV curves for the unirradiated structure, i.e., zero traps. Anode current in logarithmic scale.

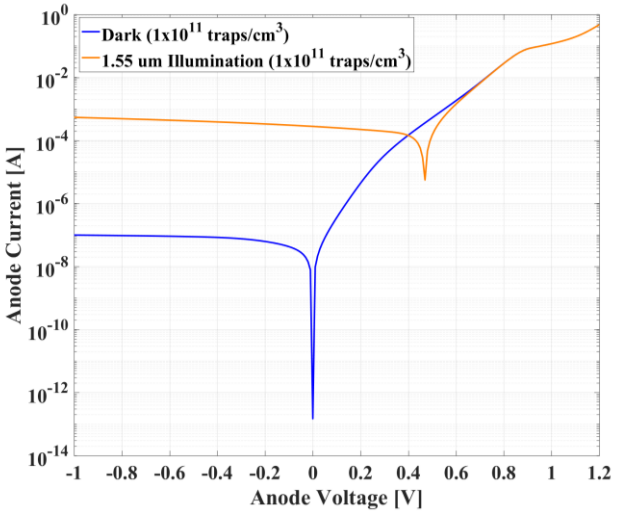

Fig. 9. Simulated dark and illuminated IV curves for a structure having uniform spatial density of 1×10^{11} traps/cm^3 at midgap energy for both the InGaAs and InP regions. Anode current in logarithmic scale.

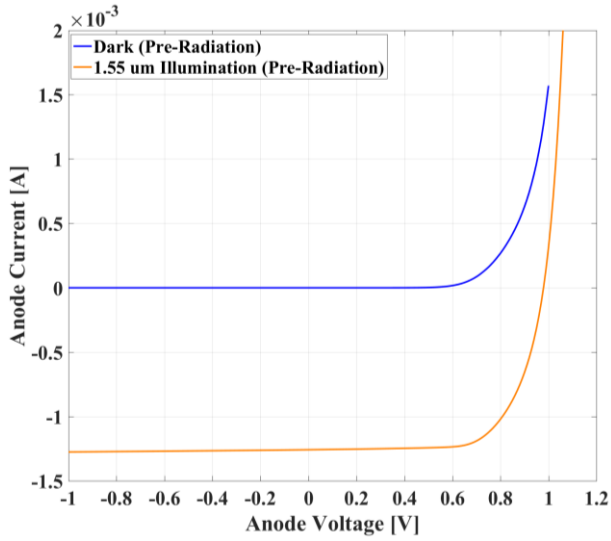

Fig. 10. Simulated dark and illuminated IV curves for the unirradiated structure, i.e., zero traps. Anode current in linear scale (Linear scale version of Fig. 8).

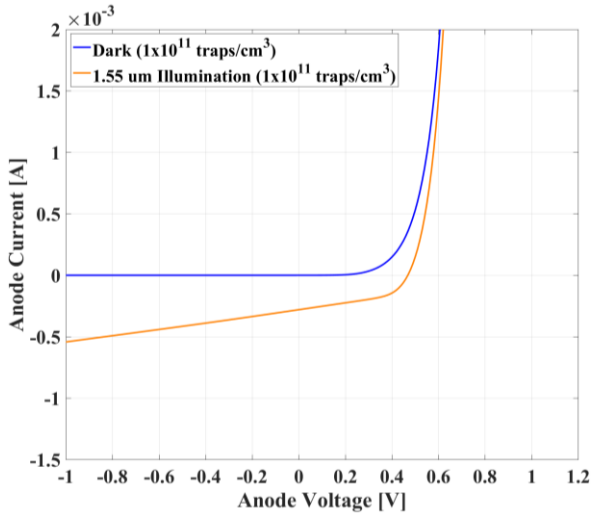

Fig. 11. Simulated dark and illuminated IV curves for a structure having uniform spatial density of 1×10^{11} traps/cm^3 at midgap energy for both the InGaAs and InP regions. Anode current in linear scale (Linear scale version of Fig. 8).

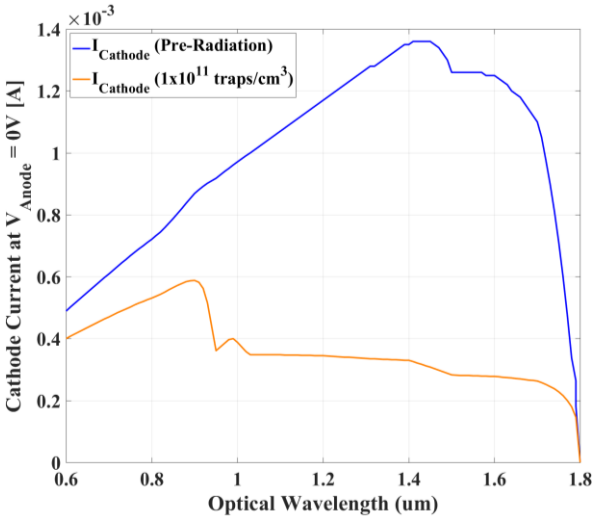

Fig. 12. Simulated responsivity as a function of optical wavelength with and without the introduction of bandgap defects into the model structure.

Figure 13 and Figure 14 examines the role of radiation-induced enhancement to the recombination rate in the structure. It appears the response is dominated by recombination in the absorption layer.

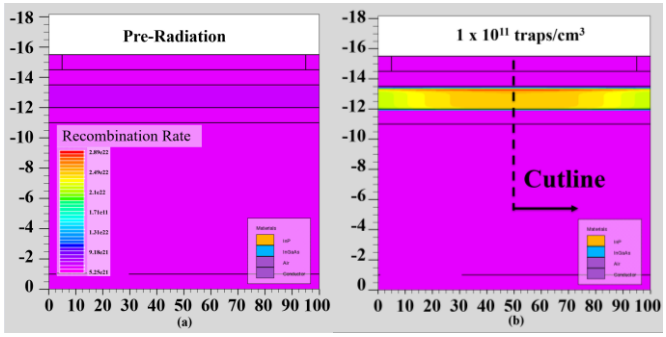

Fig. 13. Spatial distribution of the recombination rate for pre-radiation structure (Left) and post radiation (Right) modeled with a spatially uniform trap density of 1×10^{11} traps/cm^3.

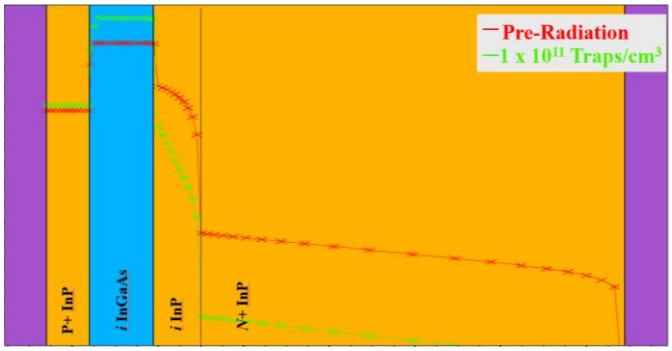

Fig. 14. Pre- and post-radiation recombination rate plotted along a vertical cutline in the center of the model structure.

Figures 15 illustrates a higher-level SPICE simulation which will be modified to incorporate post-rad behavior of the diode in the future work.

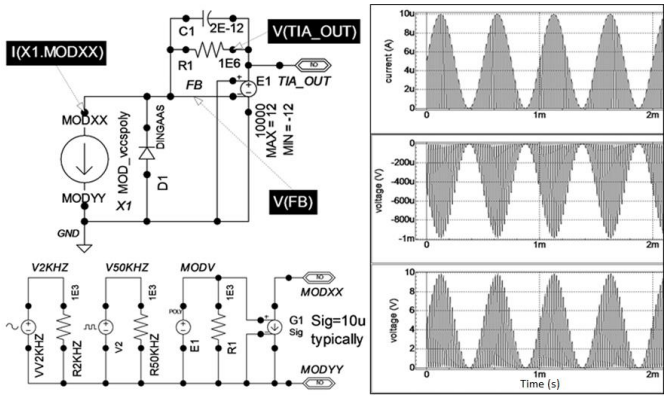

Fig. 15. (Top Left) SPICE macro model of the InGaAs diode operated in photovoltaic configuration with a Transimpedance amplifier. (Bottom Left) SPICE approach to micromodel for the modulated optical waveform. (Right) SPICE simulation results for a pre-radiation diode model.

VI. Conclusion

Proton-irradiated InGaAs PIN diodes were irradiated with 105 MeV proton radiation with fluence levels ranging from 5.0×10^{9} p/cm^2 to 2.55×10^{11} p/cm^2. Photodiode dark current at $1V_R$ linearly increased with increasing proton fluence levels. For average dark current at $1V_R$ for DUT #4, an annealing of ~3.86% (±2.73) was observed after 56 days of room temperature, unbiased storage.

The InGaAs photodiodes exhibit increased dark current consistent with displacement damage. These phenomena were explored further in TCAD simulations of dark current and responsivity by incorporating a spatially uniform distribution of trap states into device model. A preliminary SPICE model for the device operating in photovoltaic mode circuit application is also presented. We plan to continue the model development with pre- and post-radiation mixed mode simulations. Additional model refinement may include less simplified assumptions about the radiation-induced defect population, for example, surface defects as well as bulk defects.

VII. Acknowledgment

This work was supported by the Facebook Connectivity Lab.

VIII. References

[1] Hamamatsu Photonics K.K., Solid State Division. “InGaAs PIN photodiode G6849 series.” PDF Datasheet (2013).

[2] Barde, S., et al. "Displacement damage effects in InGaAs detectors: experimental results and semi-empirical model prediction." IEEE Transactions on Nuclear Science 47.6 (2000): 2466-2472.

[3] Troska, Jan, et al. “Neutron, proton and gamma radiation effects in candidate InGaAs pin photodiodes for the CMS tracker optical links.” No. CERN-CMS-NOTE-1997-102. 1997.

[4] http://www.laserfocusworld.com/articles/print/volume-46/issue-9/features/ultrafast-detectors.html